BJ www.biochemj.org

BJ Cell

Biochem. J. (2012) **442**, 661–670 (Printed in Great Britain) doi:10.1042/BJ20111745

online data

A cohesin–RAD21 interactome

Anil K. PANIGRAHI, Nenggang ZHANG, Subhendu K. OTTA and Debananda PATI[1]

Texas Children's Cancer Center, Department of Pediatric Hematology/Oncology, Baylor College of Medicine, 1102 Bates Avenue, Suite 1220 Houston, TX 77030, U.S.A.

The cohesin complex holds the sister chromatids together from S-phase until the metaphase-to-anaphase transition, and ensures both their proper cohesion and timely separation. In addition to its canonical function in chromosomal segregation, cohesin has been suggested by several lines of investigation in recent years to play additional roles in apoptosis, DNA-damage response, transcriptional regulation and haematopoiesis. To better understand the basis of the disparate cellular functions of cohesin in these various processes, we have characterized a comprehensive protein interactome of cohesin–RAD21 by using three independent approaches: Y2H (yeast two-hybrid) screening, immunoprecipitation-coupled-MS of cytoplasmic and nuclear extracts from MOLT-4 T-lymphocytes in the presence and absence of etoposide-induced apoptosis, and affinity pull-down assays of chromatographically purified nuclear extracts from pro-apoptotic MOLT-4 cells. Our analyses revealed 112 novel protein interactors of cohesin–RAD21 that function in different cellular processes, including mitosis, regulation of apoptosis, chromosome dynamics, replication, transcription regulation, RNA processing, DNA-damage response, protein modification and degradation, and cytoskeleton and cell motility. Identification of cohesin interactors provides a framework for explaining the various non-canonical functions of the cohesin complex.

Key words: apoptosis, cohesin, RAD21, sister chromatid cohesion.

INTRODUCTION

The sister chromatids generated in S-phase must stay cohered in order to facilitate chromosomal bi-orientation prior to segregation into the daughter cells. Such cohesion between the sister chromatids is mediated by the tripartite cohesin ring, formed by two SMC (structural maintenance of chromosome) proteins SMC1A and SMC3, and the α-kleisin subfamily protein RAD21 [1–3]. Another non-SMC SA (stromal antigen) protein (one of SA1, SA2 and SA3), a homologue of the budding yeast Scc3p, also is associated invariably with, and is considered an integral component of, the cohesin ring [4,5]. At different stages of the cell cycle, several other proteins also dynamically associate with cohesin and regulate both cohesion and separation of sister chromatids; these include sororin/CDCA5 (cell-division-cycle-associated 5), PDS5A and PDS5B, WAPAL (wings apart-like homologue), SGOL1 (shugoshin-like 1) and separase [6–8]. In early prophase of the vertebrate cell cycle, cohesin is removed from the chromosomal arms in a reaction dependent on the kinase PLK1 (polo-like kinase 1) and the cohesin interactor WAPAL [9–11]. Once the chromosomes are properly bi-orientated, the residual cohesin from the centromeres is removed in a reaction dependent on proteolytic cleavage of RAD21 by the endopeptidase separase [9,12]. Altered expression of both separase and RAD21 [13–16], as well as inactivating mutations in cohesin component SA2 [17] can lead to genomic instability and have been implicated in tumorigenesis ([13,14,16,18,19]; see [20] for a recent review).

Apart from co-ordination of sister chromatid cohesion and separation, the cohesin complex has also been shown to contribute to various other chromosomal functions [6,21], including gene regulation [22–24]. Horsfield et al. [25] reported a mutant strain of zebrafish, Nz171, which lacks all haematopoietic RUNX1 (Runt-related transcription factor 1) expression in early embryogenesis and demonstrates defective haematopoiesis. They determined that the gene underlying Nz171 was *rad21*. These findings provide evidence that cohesin plays a role in haematopoiesis and development. Subtle mutations in cohesin components that apparently do not affect the chromosomal cohesion can cause an altered transcriptome and have been associated with human diseases [22]. Furthermore, cohesin also plays important roles in the DDR (DNA-damage response) pathway [26,27]. Whereas post-replicative recruitment of cohesin is important for the repair of DNA double-strand breaks [28], RAD21 haploinsufficiency confers a DNA-damage defect and sensitivity to ionizing radiation [29]. Investigations over the past few years have also shed significant light on the role of cohesin in DNA replication [30]. Cohesin directly interacts with proteins involved in DNA replication [31], organizes the architecture of replicating chromatin [32] and accelerates replication processivity [33]. In addition to the various critical roles it plays in chromosome biology, cohesin is involved in apoptosis. The cohesin component RAD21 is cleaved during apoptosis [29,34], and the C-terminal fragment of RAD21 is thought to translocate to the cytoplasm to accelerate the apoptotic response [34].

Abbreviations used: CAPN1, calpain-1; CDC34, cell division cycle 34; CDCA5, cell-division-cycle-associated 5; CE, cytosolic extract; CHD, chromodomain helicase DNA-binding protein; CT, C-terminal; CTl, CT long; CTs, CT short; CUL4A, cullin 4A; DAPK3, death-associated protein kinase 3; DAVID, the database for annotation, visualization and integrated discovery; DBC1, deleted in breast cancer protein 1; DDB1, DNA damage-binding protein 1; DDR, DNA-damage response; DHX9, DEAH (Asp-Glu-Ala-His) box polypeptide 9; DISC1, disrupted in schizophrenia 1; EWS1, Ewing's sarcoma 1; FBS, fetal bovine serum; FEN1, Flap endonuclease 1; FHL3, four and a half LIM domains 3; FL, full-length; GADD34, growth arrest and DNA damage-inducible protein 34; Gal4AD, Gal4 activation domain; HA, haemagglutinin; HEK, human embryonic kidney; KPNB1, karyopherin (importin) β1; LC-MS/MS, liquid chromatography-coupled tandem MS; MCM, minichromosome maintenance complex component; NCAPG, non-SMC condensin I complex subunit G; NE, nuclear extract; NT, N-terminal; NUMA, nuclear mitotic apparatus protein; ORF, open reading frame; PCNA, proliferating cell nuclear antigen; PPM1D, protein phosphatase 1D; RFC, replication factor C; SA, stromal antigen; SMC, structural maintenance of chromosome; SRRM1, serine/arginine repetitive matrix 1; STRING, search tool for the retrieval of interacting genes/proteins; THOC4, THO complex component 4; TNFR, TNF (tumour necrosis factor) receptor; TPR, translocated promoter region; UBA1, ubiquitin-activating enzyme 1; WAPAL, wings apart-like homologue; WCL, whole cell lysate; YBX1, Y box-binding protein 1; Y2H, yeast two-hybrid.

[1] To whom correspondence should be addressed (email pati@bcm.tmc.edu).

How cohesin co-ordinates such diverse functions in the cell is not clear. A simple notion would posit that cohesin physically interacts with various proteins within disparate cellular microenvironments to regulate diverse cellular functions, and identification of a cohesin interactome would shed light on the mechanisms of cohesin function. To test the above hypothesis, we have attempted to characterize comprehensively the cohesin–protein interactome in human cells. We took three independent approaches: a Y2H (yeast two-hybrid) screen with RAD21 as the bait, an immunoprecipitation-coupled-MS analysis for RAD21-bound proteins and a RAD21 affinity pull-down assay to identify RAD21-interacting proteins. The results of the present study reveal a number of novel protein interactors of RAD21, with a known or projected role in pathways as diverse as chromosome dynamics, mitosis, apoptosis, DNA repair, splicing, protein translation and degradation, cytoskeleton function and metabolism. Several of these interactors have a known role in carcinogenesis.

MATERIALS AND METHODS

Y2H screen

The screen was conducted as described elsewhere [35]. FL (full-length; amino acids 1–631), NT (N-terminal; amino acids 1–282), CTl (C-terminal long; amino acids 254–631) and CTs (C-terminal short; amino acids 283–631) versions of the *RAD21* ORF (open reading frame) were sub-cloned in-frame with the Gal4DBD (Gal4 DNA-binding domain) in a pPC97 vector (bait). An activated human T-cell cDNA library in a Gal4AD (Gal4 activation domain) fusion vector pPC86 was used as prey in the screening along with the baits. More than 3×10^6 colonies were screened for each transformation.

Cell culture and transfection

MOLT-4 cells were grown in RPMI 1640 with 10 % FBS (fetal bovine serum). HeLa and HEK (human embryonic kidney)-293T cells were grown in DMEM (Dulbecco's modified Eagle's medium) plus 10 % FBS. FLAG- (pFlag CMV2), HA (haemagglutinin)- (pCruz-HA) and Myc- (pCS2MT) tagging vectors were used to generate the expression constructs for the selected proteins and transfected into HEK-293T cells using the calcium phosphate method as described previously [11]. When applicable, MOLT-4 cells were treated with 25 μM etoposide for 4 h (for the RAD21 cleavage assay and affinity pull-down experiments, see below) or with 10 μM for 12 h (for immunoprecipitation-coupled-MS identification of RAD21 interactors).

Cell fractionation and immunoprecipitation-coupled-MS

CEs (cytoplasmic extracts) were prepared by hypotonic lysis of cells with HB [hypotonic buffer; 10 mM Tris/HCl (pH 7.8), 10 mM NaCl and 1.5 mM $MgCl_2$ supplemented with 0.2 % Nonidet P40] into cytoplasmic and nuclear fractions. Nuclear pellets were extracted [NE (nuclear extract)] with NETN buffer [25 mM Tris/HCl (pH 7.8), 150 mM NaCl, 1mM EDTA and 0.5 % Nonidet P40]. Total soluble proteins were prepared by extracting cells with NETN buffer. The residual pellet was resuspended in NETN buffer and fragmented by sonication (for a total of 5 min at setting 2.5 in a Sonic Dismembrator 550, Fisher Scientific) to prepare the chromatin fraction. Cellular fractions were immunoprecipitated with an anti-RAD21 antibody as described previously [36]. The immunoprecipitated proteins were resolved by SDS/PAGE (10%), and gel slices were processed for tryptic digestion and LC-MS/MS (liquid chromatography-coupled tandem MS) analysis by the Proteomics Core Facility at Baylor College of Medicine, Houston, TX, U.S.A.

Antibodies and Western blotting

Western blotting was performed as described previously [37]. Rabbit polyclonal and mouse monoclonal antibodies against RAD21 have been described previously [34]. The following other antibodies were used at the dilutions indicated: anti-HA (H6908; 1:10000) and anti-DAPK3 (death-associated protein kinase 3)/Zip kinase (Z0134; 1:1000) were from Sigma–Aldrich; anti-CDC34 (cell division cycle 34) (C25820; 1:1000) was from Transduction Laboratories; anti-PPM1D (protein phosphatase 1D) (A300-664A; 1:1000), anti-SMC2 (A300-058A; 1:2000), anti-NCAPG (non-SMC condensin I complex subunit G) (A300-602A; 1:2000), anti-DDB1 (DNA damage-binding protein 1) (A300-462A-1; 1:1000), p30/DBC1 (deleted in breast cancer protein 1) (A300-434A; 1:4000) and anti-EWS1 (Ewing's sarcoma 1) (A300-417K; 1:5000) were from Bethyl Laboratories; anti-tubulin (CP06-100UG; 1:5000) was from Oncogene Research Products; anti-lamin B (ab16048; 1:2000) was from Abcam; anti-SMC1A (sc-10707; 1:1000) and anti-GADD34 (growth arrest and DNA damage-inducible protein 34) (sc-8327; 1:000) were from Santa Cruz Biotechnology; and anti-UBA1 (ubiquitin-activating enzyme 1) (NB600-472; 1:1000) was from Novus Biologicals.

Assay and partial purification of RAD21 cleavage activity

Myc–RAD21 substrate was synthesized from pCS2MT-RAD21 plasmid in a wheat-germ extract-based TNT® (Promega) reaction. NEs from apoptotic MOLT-4 cells were prepared as described above, but in a different buffer [PP buffer-300; 25 mM Tris/HCl (pH 8.0), 5 % glycerol, 1.5 mM $MgCl_2$ and 0.2 % Nonidet P40, supplemented with 300 mM NaCl]. For the RAD21 cleavage assay, NEs and fractions from chromatographic steps (see below) were incubated with Myc–RAD21 for 2 h at 37 °C and were analysed by Western blotting using an anti-RAD21 antibody which recognizes the C-terminus. The active fractions generated a 64 kDa band reminiscent of *in vivo* apoptotic fragmentation, as described previously [34]. For partial purification of the RAD21 cleavage activity, NE was diluted 1:3 with PP buffer-0 (PP buffer with no NaCl) and passed through a Uno Q1 column (1 ml, Bio-Rad Laboratories). The flow-through was bound to and eluted from a Uno S1 column (1 ml, Bio-Rad Laboratories) in a 0.1–0.5 M NaCl gradient in PP buffer. Active fractions showing RAD21 cleavage activity were pooled, concentrated and fractionated on a Superdex 200 column in PP buffer-150 (PP buffer with 150 mM NaCl). The chromatographic operations were performed using a BioLogic DuoFlow system FPLC (Bio-Rad Laboratories).

Affinity pull-down analysis

RAD21 matrix was generated by immobilizing Myc–RAD21 (from the TNT® reaction) on to anti-Myc agarose beads. The active fraction #30 from the Superdex 200 column was pre-cleared with anti-Myc agarose beads and then bound to anti-Myc agarose beads (mock) or RAD21 matrix. The beads were washed with PP buffer-150 and resolved by SDS/PAGE (8%). The entire gel was stained with Coomassie Blue and cut into slices. LC-MS/MS was performed on the all of the gel slices by Nextgen Sciences.

Bioinformatic analysis

Identified proteins were analysed using publicly available DAVID (database for annotation, visualization and integrated

Table 1 RAD21 interactors identified from Y2H screening

In total, 21 ORFs were identified from the Y2H screening using FL or NT human RAD21. UniProt accession numbers for the corresponding ORFs are listed.

RAD21 bait	Identified proteins	UniProt accession number	Processes
FL	SMC1A	Q14683	Sister chromatid cohesion, DDR, mitosis
FL	CDC34	P49427	Protein modification, protein degradation
FL	RPL13	P26373	Protein synthesis
FL	RPL10	P27635	Protein synthesis
FL	WNT2B/Wnt13	Q93097	Developmental signalling
FL	HNRNPH2/FTP-3	P55795	Splicing/RNA processing
FL	PPP1R15B	Q5SWA1	Protein modification, transcription regulation
FL	PPP1R15A/GADD34	O75807	Apoptosis, translation regulation
FL	DAPK3	O43293	Mitosis, regulation of apoptosis
FL	ZNF80	P51504	Putative transcription factor
FL	TNFRSF14	Q8N634	Apoptosis, immune response
FL	TMSB4X	P62328	Cytoskeleton/cell motility
FL	COX2	P00403	Metabolism
FL	IL7R	P16871	Immune response
FL	Cystatin-B	P04080	Proteinase inhibitor, regulation of apoptosis
FL	Filamin B	O75369	Cytoskeleton/cell motility
FL	Cofilin1	P23528	Cytoskeleton/cell motility
FL	MSRB2/CBS1	Q9Y3D2	Methionine metabolism
NT	FHL3	Q13643	Transcription, cytoskeleton/cell motility
NT	DYNLT1/TCTEL1	P63172	Cytoskeleton/cell motility, intracellular transport
NT	RPL35A	P18077	Protein synthesis

discovery) for functional classification [38]; functional annotation clustering of the list of RAD21 interactors was performed with medium classification stringency. The protein–protein interaction network was visualized using STRING (search tool for the retrieval of interacting genes/proteins) [39]. STRING presents each protein node as a circle, the size of which is automatically generated; the larger size only reflects that there is structural information associated with the protein. When available, the structure of the protein is embedded as a thumbnail within the circle. Multiple protein IDs (UniProt accession numbers) were analysed with medium confidence setting (0.400). Gene/protein identity mapping was performed manually or at Uniprot (http://www.uniprot.org). The lists of interactors were examined using the MEROPS database to identify a protease (http://merops.sanger.ac.uk/).

RESULTS

Y2H screening

We have reported previously that RAD21 is cleaved at Asp^{279} by an unknown caspase-like protease during apoptosis, and the CT (C-terminal) fragment (amino acids 283–631) translocates to the cytoplasm to further aid in the apoptotic response [34]. Therefore we were interested in finding protein interactors that specifically bind the NT or the CT fragments of RAD21. RAD21 also has a region (amino acids 257–360) with strong homology with TNFR [TNF (tumour necrosis factor) receptor], a member of the TNFR superfamily with a known role in mediating apoptosis. Since the mechanism of RAD21-mediated instigation of the apoptotic response is unknown, we hoped that inclusion of this 257–360 amino acid region might also identify some specific interactors. Therefore we used two versions of CT RAD21 as baits.

The screen using FL RAD21 identified 18 positive clones, whereas the screen with NT RAD21 identified three positive clones (Table 1), and all of these clones were in-frame with the Gal4AD. We obtained several positive clones with the CTl and CTs RAD21 screens, but none was in-frame with the Gal4AD. The validity of the screening result is reflected by the identification of SMC1A as a RAD21 interactor. SMC1A joins with RAD21 and SMC3 to form the tripartite ring of the mitotic cohesin complex. Our screen also identified several RAD21 fragments as RAD21 interactors, indicating self-association of RAD21 molecules, which has been described previously [36], and further confirming the validity of this Y2H screen. Of the total 21 ORFs identified, all but SMC1A are novel interactors of RAD21. Functional annotation analysis performed using DAVID revealed five proteins that are involved in apoptosis: DAPK3, PPP1R15A/GADD34, TNFRSF14, CSTB (cystatin B) and CFL1 (cofilin 1). The other proteins identified are involved in diverse processes, including protein synthesis, protein degradation, splicing, transcription and signalling. We reconfirmed the interactions in candidate-specific Y2H experiments (results not shown). As an alternative validation, we generated epitope-tagged versions of some of the identified ORFs, co-expressed them in HEK-293T cells along with RAD21, and performed immunoprecipitation experiments. As shown in Figure 1, RAD21 physically interacts with FHL3 (four and a half LIM domains 3) (Figure 1A), CDC34 (Figure 1B) and DAPK3 (Figure 1D).

Additionally, we took a candidate-based approach to find novel RAD21 interactors. One such candidate is the phosphatase Wip1/PPM1D, which functions in the DDR pathway. PPM1D has also been suggested to dephosphorylate SMC1A [40]. Therefore we wanted to verify its interaction with RAD21. As shown in Figure 1(C), PPM1D and RAD21 interact when overexpressed.

Immunoprecipitation-coupled-MS analysis

Our Y2H assay identified a few RAD21-interacting proteins that could only be validated using overexpressed proteins. Considering the inherent drawbacks of the Y2H assays, including overexpression of the constructs and potential for false positives/negatives, we embarked on a biochemical approach to identify physiological interactors of RAD21 using endogenous RAD21 immunoprecipitaton followed by MS analyses. We performed several immunoprecipitation experiments using an antibody raised against the CT of RAD21 [34] (see the schematic diagram in Figure 2A). First, RAD21 was immunoprecipitated

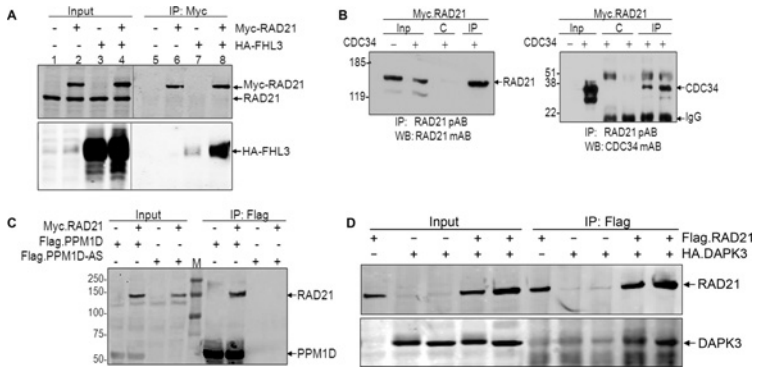

Figure 1 Validation of the RAD21 interaction with candidates identified in the Y2H screen

(**A**) Myc-tagged RAD21 and HA-tagged FHL3 proteins were expressed in HEK-293T cells as indicated, and immunoprecipitation was performed using anti-Myc agarose. RAD21 pulls down FHL3 (lane 8). (**B**) Myc-tagged RAD21 and untagged CDC34 were expressed in HEK-293T cells as indicated, and immunoprecipitation was performed using an anti-RAD21 polyclonal antibody (RAD21 pAb). The immunoprecipitates were analysed by Western blotting (WB) using an anti-RAD21 mouse monoclonal antibody (RAD21 mAb) and an anti-CDC34 mouse monoclonal antibody. (**C**) Myc-tagged RAD21 is pulled down by FLAG-tagged PPM1D, but not by an anti-sense construct PPM1D-AS, when expressed in HEK-293T cells. (**D**) FLAG-tagged RAD21 pulls down HA-tagged DAPK3 in HEK-293T cells. Each dividing line indicates that unrelated intervening lanes were spliced. The molecular mass in kDa is indicated on the left-hand side. C, control; Inp, input; IP, immunoprecipitation.

from the CEs prepared from normal as well as MOLT-4 apoptotic acute lymphoblastic leukaemia cells. As previously shown [34], RAD21 is normally a nuclear protein, but is cleaved during apoptosis and its CT fragments translocate to the cytoplasm (see Figure 2B, compare lane 1 with lane 2). Immunoprecipitation from the untreated CEs was thus considered both as a negative control for the immunoprecipitation and as a tool to access sticky proteins that might cross-react with the anti-RAD21 antibody. The immunoprecipitates were subjected to mass spectrometric analyses to identify the proteins. All four canonical components of the cohesin complex (RAD21, SMC1A, SMC3 and SA2) were identified in the immunoprecipitate from the apoptotic CEs, whereas no cohesin components were detected in the immunoprecipitate from the etoposide-untreated CEs (Supplementary Table S1 at http://www.BiochemJ.org/bj/442/bj4420661add.htm). Several proteins were also detected only in the immunoprecipitate from the cohesin-deficient untreated CEs, indicating that they somehow cross-react with anti-RAD21 antibody (Supplementary Table S1). These proteins were therefore considered non-specific and were excluded from further analysis. We also prepared CEs and NEs from HeLa cells and performed immunoprecipitation using an anti-RAD21 antibody. RAD21 is usually not present in the cytosol (Figure 2B), and thus the immunoprecipitation from HeLa CEs served as an additional negative control. We identified in the NE immunoprecipitate all components of the canonical cohesin complex, known cohesin-associated proteins including PDS5A and WAPAL, as well as novel cohesin-interactors including Nap1L1 (nucleosome assembly protein 1-like 1), RFC (replication factor C) 3 and condensin component NCAPG (see Supplementary Table S2 at http://www.BiochemJ.org/bj/442/bj4420661add.htm). However, no cohesin component was detected in the immunoprecipitate from the CEs.

Because RAD21 and the cohesin complex exist in the cell both as a soluble pool and as a chromatin-bound fraction, and the only other proteolytic processing of RAD21 known to occur is during apoptosis, our aim was to identify RAD21 interactors from total soluble proteins and from the insoluble chromatin-enriched fraction from cells treated with or without etoposide. Table 2 lists the proteins identified from the immunoprecipitates from both the soluble and chromatin fractions. Proteins with two or more peptides retrieved from the MS were taken into consideration. This analysis detected all of the components of the canonical cohesin complex as well as the known cohesin interactors PDS5A, PDS5B and WAPAL that regulate both the chromatin–cohesin interaction and the resultant sister chromatid cohesion. Additionally, this analysis also revealed several novel interactors that supposedly function in a microenvironment related to cohesin. For example, cohesin has been shown to be important for the DDR [34,35], and our analysis identified DDB1 as a RAD21 interactor. The replication licensing and execution machinery, along with the clamp PCNA (proliferating cell nuclear antigen) and various RFC complexes (loader and unloader of the PCNA clamp), have been proposed to function in conjunction with cohesin and cohesion establishment. We identified several replication licensing factors [MCM (minichromosome maintenance complex component) 2, MCM3, MCM4 and MCM7 isoform 1 and 2], as well as PCNA as RAD21 interactors, whereas identification of RFC3 has been mentioned above. Interestingly, our analysis also identified the chromodomain ATPase CHD (chromodomain helicase DNA binding protein) 4/Mi2β as a novel interactor of RAD21. CHD4 is highly similar to CHD3/Mi2α, which is a known interactor of RAD21 [41]. Apart from these, several other proteins were also identified as novel RAD21 interactors that supposedly function in a wide variety of cellular pathways (see Table 2).

We used the STRING database [39] to analyse all of the RAD21 interactors, excluding contaminating proteins (Figure 2C). STRING plots the listed proteins (nodes) based on the strength of internodal interactions, which is comprised of protein–protein binding (black lines) as well as functional interactions other than binding (grey lines). In the present study, we included five highly predicted proteins in the analysis that are selected automatically by the program based on the input list of proteins. The five proteins automatically added to this list include FEN1 (Flap endonuclease 1), CDKN1A (cyclin-dependent kinase inhibitor 1A), RFC1 and DDB1-interacting partners CUL4A (cullin 4A) and DDB2 (all underlined; Figure 2C). Our analysis predicts cohesin components SMC1A and SMC3 to interact with FEN1, RFC1 and PCNA, whereas PCNA would further link with the replication licensing factors (Figure 2C). Importantly, we later identified both FEN1 and CUL4A as specific RAD21 interactors in a different experiment with an independent approach (see below). Another interesting observation is the physical interaction of transcription regulator THOC4 (THO complex component 4) with RAD21. THOC4 has been found to interact with SMC1A

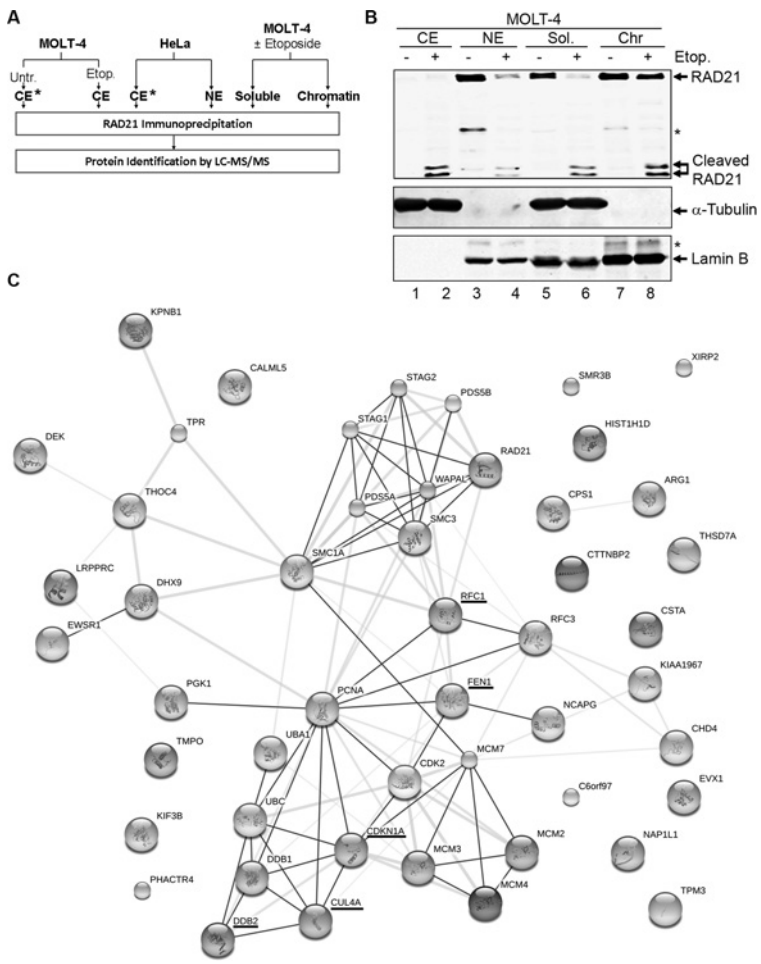

Figure 2 RAD21 interactors as identified by immunoprecipitation-coupled-MS

(**A**) A schematic diagram for RAD21 immunoprecipitation-coupled MS experiments. In a parallel experiment, total soluble proteins (soluble) were prepared by extracting MOLT-4 cells with NETN buffer; the residual pellet was sonicated to release the chromatin fraction. The asterisk indicates a RAD21-negative pool. (**B**) Cellular fractionation of MOLT-4 cells. Fractionation of MOLT-4 into CEs and NEs, and into soluble proteins (Sol.) and chromatin (Chr.) were performed in two independent experiments. α-Tubulin and lamin B were used as markers of cytoplasmic (CE) and nuclear (NE) fractions respectively. Non-specific bands are marked by asterisks. (**C**) Protein identifiers were analysed with STRING, with a setting of medium confidence (0.400). Five most predictable interactors (underlined) were automatically added by selecting 'no more than five interactors' for additional 'interactors shown'. Black internodal lines indicate known binding, whereas grey lines indicate known or predicted functional interactions other than direct binding. Proteins that are discussed in more detail are defined in the text or in the Tables, other protein abbreviations used in this Figure have not been defined.

[42]. THOC4 also interacts with TPR (translocated promoter region) and the importin KPNB1 [karyopherin (importin) β1], the nuclear pore and nuclear transport components that we also found to physically interact with RAD21. Three distinct hubs are apparent in the STRING analysis: cohesin and cohesin-related proteins, UBC, DDB1 and UBA1-related ubiquitin–proteasome pathway proteins, and the MCM-RFC-related pro-replication proteins. This finding is significant because cohesin has been implicated in both replication and the DDR.

As shown in Figure 3, several of the interactors were experimentally validated for their interaction with RAD21 using endogenous protein immunoprecipitation. They include DDB1, p30/DBC1/KIAA1967, PPP1R15A/GADD34 and EWS1 (Figure 3A). We observed that both DDB1 (which is part of the CUL4A ubiquitin ligase complex) and the ubiquitin-activating enzyme UBA1 (E1) bind to RAD21 and to each other (Figure 3B). We also observed UBA1, EWS1 and DDB1 immunoprecipitating each other (results not shown), the biological significance of which is currently under investigation. Figure 3(C) further demonstrated that RAD21 and p30/DBC1 can co-immunoprecipitate each other.

Affinity pull-down analysis

RAD21 is proteolytically cleaved during mitosis by the endopeptidase separase [12], but the identity of the protease responsible for the apoptotic cleavage of RAD21 is unclear [34]. In our immunoprecipitation-coupled-MS investigations into RAD21 interactors, as described above, we did not identify any protease that interacted with RAD21. Therefore we used an affinity pull-down approach geared towards identifying a RAD21 protease and additional RAD21-binding proteins during apoptosis. We generated a RAD21 affinity matrix by immobilizing *in-vitro*-translated Myc–RAD21 on to anti-Myc agarose beads. RAD21-cleaving activity in the apoptotic NEs from MOLT-4 cells was enriched over three chromatographic steps and finally was bound to the RAD21 matrix as well as to anti-Myc agarose beads (see the schematic diagram in Figure 4A, and RAD21 cleavage assay in Figure 4B). The bound proteins were subjected to LC-MS/MS analysis. Supplementary Table S3 (at http://www.BiochemJ.org/bj/442/bj4420661add.htm) lists all 97 proteins that specifically bound to the Myc–RAD21 matrix, but not to the Myc beads (Mock), for which a minimum

Table 2 Identification of RAD21 interactors from immunoprecipitation-coupled-MS

Immunoprecipitation was performed with soluble (Sol.) and chromatin (Chr.) fractions from normal (untreated) and apoptotic (etoposide-treated) MOLT-4 cells.

		Untreated*		Etoposide*			
Proteins	Description	Sol.	Chr.	Sol.	Chr.	UniProt accession number	Processes
RAD21	Double-strand-break repair protein RAD21 homologue	583	478	321	161	O60216	Sister chromatid cohesion, DDR, mitosis
SMC1A	Structural maintenance of chromosomes protein 1A	527	475	759	606	Q14683	Sister chromatid cohesion, DDR, mitosis
SMC3	Structural maintenance of chromosomes protein 3	647	626	916	919	Q9UQE7	Sister chromatid cohesion, DDR, mitosis
SA1	Cohesin subunit SA-1	41	30	76	79	Q8WVM7	Sister chromatid cohesion, DDR, mitosis
SA2	Cohesin subunit SA-2	276	134	411	280	Q8N3U4	Sister chromatid cohesion, DDR, mitosis
PDS5B	Sister chromatid cohesion protein PDS5 homologue B	80	8	79	14	Q9NTI5	Sister chromatid cohesion, mitosis
WAPAL	Wings apart-like (*Drosophila*)	98	27	22	4	Q7Z5K2	Sister chromatid cohesion, mitosis
PHACTR4	Phosphatase and actin regulator 4 isoform 2	15	4	7	4	Q8IZ21	Protein modification, cytoskeleton/cell motility
UBC	Ubiquitin C	2	1		4	P0CG48	Protein modification, protein degradation
TPM3	Tropomyosin 3	14	1			P06753	Cytoskeleton/cell motility
KPNB1	Karyopherin (importin) β1	2	4			Q14974	Nucleocytoplasmic trafficking
C6orf97	Hypothetical protein LOC80129; FLJ23305	12	2			Q8IYT3	Uncharacterized
UBA1	Ubiquitin-activating enzyme E1	6		10	1	P22314	Protein modification, protein degradation
DDB1	Damage-specific DNA-binding protein 1, 127 kDa	39		8		Q16531	DDR, protein degradation
MCM2	DNA replication licensing factor MCM2	2			1	P49736	DNA replication
EWS1/ EWSR1	Ewing sarcoma breakpoint region 1	2			1	Q01844	Uncharacterized, transcription regulation
KIAA1967	p30/DBC protein	9				Q8N163	Apoptosis
XIRP2	Cardiomyopathy-associated protein 3	5				A4UGR9	Cytoskeleton/cell motility
CALML5	Calmodulin-like skin protein		6			Q9NZT1	Calcium signalling, development
DEK	Protein DEK isoform 1			8		P35659	Transcription regulation
THSD7A	Thrombospondin type-1 domain-containing protein			5		Q9UPZ6	Uncharacterized
SMR3B	Submaxillary gland androgen-regulated protein 3B	2				P02814	Extracellular processes
PDS5A	Sister chromatid cohesion protein PDS5 homologue A		2			Q29RF7	Sister chromatid cohesion, mitosis
THOC4	THO complex subunit 4	2				Q86V81	Splicing/RNA processing, transcription regulation
CTTNBP2	Cortactin-binding protein 2		2			Q8WZ74	Cytoskeleton/cell motility, protein modification
TPR	Nucleoprotein TPR		4		3	P12270	Mitosis, protein synthesis, nucleocytoplasmic trafficking
MCM7	DNA replication licensing factor MCM7 isoform 2		3			A4D2A2	DNA replication
MCM3	DNA replication licensing factor MCM3		2			P25205	DNA replication
MCM7	DNA replication licensing factor MCM7 isoform 1		1		1	P33993	DNA replication
MCM4	DNA replication licensing factor MCM4		1		2	P33991	DNA replication
PCNA	Proliferating cell nuclear antigen		2		1	P12004	DNA replication, mitosis
TMPO	Thymopoietin isoform γ		5		4	P42167	Transcription regulation, DNA replication, mitosis
PGK1	Phosphoglycerate kinase 1		2		4	P00558	Glycolysis
EVX1	Homeobox even-skipped homologue protein 1		2		2	P49640	Transcription regulation
CHD4	Chromodomain-helicase-DNA-binding protein 4		1		1	Q14839	Chromatin modification/ remodelling, transcription regulation

*Numbers in columns indicate peptides retrieved for each protein.

of two peptides were retrieved. This list has an enormous abundance of ribosomal proteins and translation factors. In order not to overwhelm our analysis by the abundant sticky ribosomal proteins which have been identified in many other immunoprecipitation-coupled-MS analyses, we excluded these proteins, plus HSP90A (heat-shock protein 90A) chaperone, from further consideration. These proteins are listed in Supplementary Table S3.

Since the goal of the present study was to identify a RAD21 proteinase, we first focused on the ubiquitous protease CAPN1 (calpain-1; two peptides were retrieved in the analysis). We verified that CAPN1 cleaves RAD21 *in vitro* and *ex vivo* upon calcium treatment, but not during apoptosis. The site of CAPN1 cleavage (Leu^{192}) is different from the apoptotic cleavage (Asp^{279}), and this cleavage promotes sister chromatid separation [37]. The characterization of CAPN1 as a bona fide RAD21 interactor validates our affinity-purification approach. The only other probable protease (according to the MEROPS database) identified in this experiment is the CAD protein, which actually is a fusion of four biochemical activities: GATase (glutamine amidotransferase), CPSase (carbamoyl phosphaste synthase), ATCase (aspartate carbamoyl transferase) and DHOase (dihydroorotase).

We also identified four components of the human condensin I complex, namely SMC2, SMC4, NCAPG and NCAPD2 (non-SMC condensin I complex subunit D2). NCAPG was also identified in one of the RAD21 immunoprecipitation experiments (Supplementary Table S2). Currently, a notion of physical interaction between condensin and cohesin has not been appreciated. Therefore we decided to verify whether such physical interactions between RAD21 and condensins do exist. We immunoprecipitated RAD21 from normal or apoptotic MOLT-4 WCLs (whole cell lysates) and observed two endogenous condensin I components, SMC2 and NCAPG, co-immunoprecipitating with RAD21 (Figure 4C). Interestingly, we also observed proteolytic truncation of NCAPG (marked with an asterisk; Figure 4C) in the apoptotic WCL.

Also consistent with the bioinformatic prediction as depicted in Figure 2(C), we identified the flap endonuclease FEN1 as a specific interactor of RAD21. STRING predicts interaction of FEN1 with TOP3A (topoisomerase III α) and DDB1, both of which, along with the DDB1-partner CUL4A, were identified as specific direct interactors of RAD21 in this analysis.

Analysis of this list of proteins by DAVID revealed only five proteins involved in apoptosis: RAD21 itself, CAPN1, API5 (apoptosis inhibitor 5), CUL4A and TUBB2C (tubulin β2C).

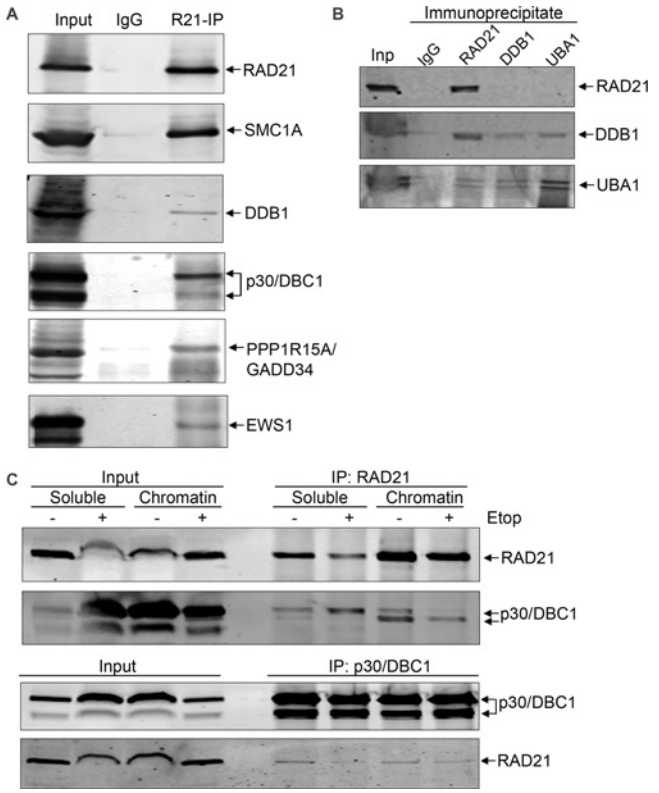

Figure 3 Validation of RAD21 interactors identified by immunoprecipitation-coupled-MS

(**A**) Endogenous RAD21 was immunoprecipitated from MOLT-4 cells and examined for the presence of proteins as indicated. (**B**) Endogenous RAD21, DDB1 and UBA1 were immunoprecipitated from MOLT-4 cells and examined as indicated. (**C**) MOLT-4 cells, untreated or treated with etoposide (10 μM, 10 h), were fractionated into total soluble proteins and chromatin fractions. Endogenous RAD21 and p30/DBC1 were immunoprecipitated and examined as indicated. Etop, etopside; Inp, input; IP, immunoprecipitation.

DISCUSSION

Cohesin has been implicated in a vast range of cellular processes apart from sister chromatid cohesion and separation. It is possible that cohesin communicates with several proteins that function in different cellular processes. For instance, cohesin interacts with the spindle pole-associated factor NUMA (nuclear mitotic apparatus protein) and co-localizes with the spindle poles [43]. The entire cohesin complex also has been reported to interact with the nuclear matrix [43,44]. Recently, cohesin has been reported to interact with AIRE (autoimmune regulator), a master regulator of the expression of peripheral tissue self-antigens [45]. Several other proteins, such as the splicing factor SKIP/SNW1 [46], the schizophrenia risk gene product DISC1 (disrupted in schizophrenia 1) [47] and the *Yersinia pestis* pathogen protein Y2928 [48], have also been suggested to interact with cohesin. However, no elaborate investigation into protein interactors of cohesin has been performed. In the present paper we report characterization of the cohesin protein interactome, which we identified by using principal cohesin subunit RAD21 as the bait.

Using three different approaches, Y2H, immunoprecipitation-coupled-MS and affinity pull-down analysis, we identified 112 novel interactors of RAD21, several of which were validated in immunoprecipitation experiments. As shown in Table 3, these proteins largely fall into ten classes, with some overlaps, on the basis of the cellular processes in which they are involved. We identify previously unsuspected processes, such as protein modification and degradation, cytoskeleton and cell motility, and RNA processing and nucleocytoplasmic trafficking, in which RAD21-interacting proteins play a role. These results suggest the involvement of RAD21 in vastly different cellular processes beyond sister chromatid cohesion and separation. Our analysis reveals several important nodal hubs of known physical interactions within the RAD21 interactome. The foremost is the cohesin complex along with its known associated proteins, condensin-I and chromatin modifiers (Figure 5A). The other important hubs identified include replication-associated proteins (Figure 5B), protein ubiquitination and deubiquitination (Figure 5C), transcription and RNA metabolism (Figure 5D), and cytoskeleton and cell motility (Figure 5E). Interestingly, the entire cohesin complex has recently been shown to interact physically with the MCM complex [32]. We analysed the entire 112 interactors using the STRING database along with 12 known RAD21 interactors (not identified from our screen): caspase 7, NUMA1, SMARCA5/SNF2H (SWI/SNF related, matrix associated, actin dependent regulator of chromatin, subfamily a, member 5), AIRE, CDCA5/sororin, CHD3/Mi2β, CHTF18/CHL12 (chromosome transmission fidelity factor 18 homologue), CTCF (CCCTC-binding factor), SRRM1/SRM160 (serine/arginine repetitive matrix 1), ESPL1/separase, DISC1 and SKIP/SNW1. Several proteins within this composite network are known to interact with each other (Supplementary Figure S1 at http://www.BiochemJ.org/bj/442/bj4420661add.htm). The replication hub appears to connect a further set of nodal hubs, including ubiquitin–proteasome pathway proteins UBC-UBA1-CUL4A-DDB1 and splicing regulators YBX1 (Y box-binding protein 1)-DHX9 [DEAH (Asp-Glu-Ala-His) box polypeptide 9]-SYNCRIP (synaptotagmin binding, cytoplasmic RNA interacting protein)-HNRNPH1 (heterogeneous nuclear ribonucleoprotein H1) (Supplementary Figure S1). DHX9 further communicates with transcription regulator THOC4, EWS1, cohesin (SMC1A) and also with the nuclear matrix protein SRRM1 (not identified in our screen). SRRM1 forms a major hub communicating with the transcription regulator THOC4, nuclear transport proteins TPR and KPNB1, and mitotic spindle stabilizer NUMA. The chromodomain chromatin remodeller CHD4 is also a transcription regulator, and appears to communicate with SRRM1, THOC4, RFCs and p30/DBC1 (Supplementary Figure S1). YBX1 is also a transcription factor important for haematopoiesis [49]. Identification of the putative transcription factor ZNF80 (zinc finger protein 80) as a RAD21 interactor may lead to important clues to cohesin's role in transcription regulation. While trying to grasp the significance of all these inter-nodal and inter-hub interactions, it is important to note that each node shown here actually interacts with cohesin (RAD21) directly.

Another point of interest depicted by the RAD21 interactome as presented in the present paper (Figure 5C) is the physical interaction of RAD21 with several components of the ubiquitin system. CDC34, which is described above as a novel RAD21 interactor (Table 1 and Figure 1B), is an E2 ubiquitin-conjugating enzyme. RAD21 also pulls down another E2 enzyme, UBE2O (ubiquitin-conjugating enzyme E2O) (Figure 5C and Supplementary Table S3). Identification of UBA1 and the E3 ligases DDB1-CUL4A and UBE3C further make a compelling case that RAD21 functions in the ubiquitin pathway. This finding is consistent with a recent report that both SMC1A and SMC3 interact with several proteins of the deubiquitination pathway [42].

One of the objectives of the present study was to understand the mechanism of RAD21-mediated apoptosis by identifying Rad21 interactors. RAD21 is cleaved during apoptosis, but the protease

Table 3 Functional classification of RAD21 interactors

Processes	RAD21 interactors
Mitosis	CDC34, CLASP2, CUL4A, NCAPD2, NCAPG, PDS5A, PDS5B, PPP1R15A, PSMC1, PSMD2, RAN, RAD21, SEPT1, SMC1A, SMC2, SMC3, SMC4, SA1, SA2, TOP3A
Chromosome dynamics	CHD4, HIST1H1D, NCAPD2, NCAPG, MCM2, NAP1L1, SMC2, SMC4, RFC3, SETD3
Replication	CDC34, MCM2, MCM3, MCM4, MCM7, RAD21, SMC1A, SMC2, SMC3, SMC4, TOP3A, RFC3, FEN1
RNA processing	HNRNPH1, SYNCRIP, LPPRC, DHX9, RAN, SKIV2L2, SMC1A, THOC4, TPR, YBX1
Transcription regulation	CDK9, CHD4, EVX1, EWS, LPPRC, MCM2, MCM3, MCM4, MCM7, NAA15, NACA3, PSPC1, RAN, YBX1, ZNF80, SETD3
Protein modification and degradation	CDC34, CPS1, CUL4A, DDB1, PSMC1, PSMD2, RN123, UBE2O, UBE3C
DDR	CUL4A, DDB1, GNL1, FEN1, MCM7, PCNA, PPM1D, SMC1A, SMC3, RAD21
Apoptosis	API5, CFL1, CUL4A, CYTB, DAPK3, P30/DBC1, PPP1R15A, TNFRSF14, TBB2C
Nucleocytoplasmic trafficking	KPNB1, NACA3, PCNA, RAN, TPR
Cytoskeleton and cell motility	ARP3, CTTN, CTTNBP2, CLASP2, CFL1, EVL, FHL3, FLNB, TPM3, TMSB4Y, DAPK3, SEPT1, KIF3B, TUBB2C
Miscellaneous	ARG1, ACAT1, C6ORF97, CPS1, CAD, CBR1

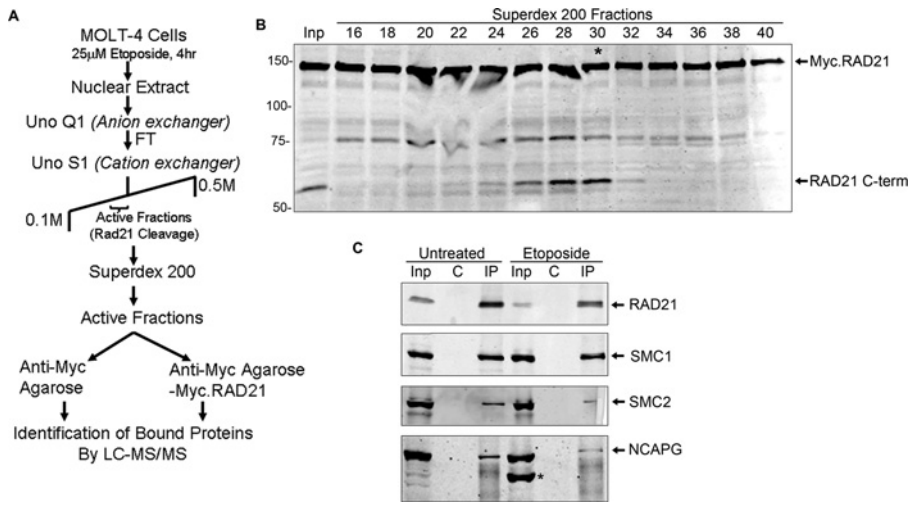

Figure 4 Affinity pull-down of proteins using Myc–RAD21 matrix

(**A**) Schematic diagram for enrichment of a RAD21-cleaving activity from apoptotic MOLT-4 cells. A total of 97 proteins were identified that bound specifically to Myc–RAD21 immobilized on anti-Myc agarose, but not to anti-Myc agarose control. Nearly half of those were ribosomal proteins or translation factors. (**B**) RAD21 cleavage assay on fractions from the gel-filtration (Superdex 200) column. Myc–RAD21, as substrate, was incubated with the pooled active fractions eluted from Uno S1 as the input, as well as the indicated fractions from the Superdex 200 column. The asterisk indicates the fraction (fraction 30) that was subsequently bound to the anti-Myc agarose and anti-Myc agarose–RAD21 matrix. The molecular mass in kDa is indicated on the left-hand side. (**C**) Endogenous RAD21 was immunoprecipated from MOLT-4 (untreated or treated with 10 μM etoposide, 10 h) WCLs and examined with anti-cohesin (RAD21, SMC1A) and anti-condensin-I (SMC2, NCAPG) antibodies. The asterisk indicates the apoptotic cleavage product of NCAPG. C, control immunoprecipitate; Inp, input; IP, RAD21 immunoprecipitate.

responsible for this cleavage remains unknown [34]. Although we were not able to identify a bona fide protease that cleaves Rad21 during apoptosis, we indentified a number of RAD21-interacting proteins with a direct or indirect role in apoptosis (see Table 3). Apoptosis requires chromatin condensation and fragmentation, and apoptotic cleavage of cohesin RAD21 is thought to play a role therein. In the present study, we uncovered the human condensin I complex as physically interacting with cohesin RAD21. This is important for two reasons. First, a notion of physical communication between cohesins and condensins did not exist until recently, when the cohesin, condensin and the chromosomal passenger complex were reported to co-operate in spindle dynamics in yeast [50]. Secondly, even though cohesin is a known proteolytic target during mitosis and apoptosis, similar proteolytic processing of a condensin component is unknown. Our observation of proteolytically cleaved condensin I component NCAPG in apoptotic WCLs raises critical questions as to why cohesin and condensin components are cleaved during apoptosis, and whether such cleavage is mechanistically linked to apoptotic chromatin condensation and fragmentation. This also emphasizes the need to identify the protease that cleaves cohesin and condensin during apoptosis. A protease–substrate interaction is meant to be transient, and the approaches taken here were inadequate to capture the protease. Use of a bioactive protein cross-linker may help in identifying the protease.

Identification of a set of novel interactors of cohesin presents enormous promise to the field of cohesin biology. The amount of information that can be generated by experimental validation of each of these interactors and elucidation of the biological significances is exemplified by CAPN1. It can be noted that CAPN1 was identified as a specific interactor of RAD21 and remains as an unconnected peripheral node (Supplementary Figure S1). However, this identification led to the discovery that CAPN1 indeed cleaves RAD21 at a precise site (Leu^{192}), causes loss of cohesin from chromatin, and consequently promotes separation of chromosomal arms [37]. Likewise, characterization of other interactors might reveal new facets of cohesin's function. However, it must be noted that the entire interactome characterization was performed using MOLT-4 cells, and the actual interactome may differ in different cell types. Moreover, it

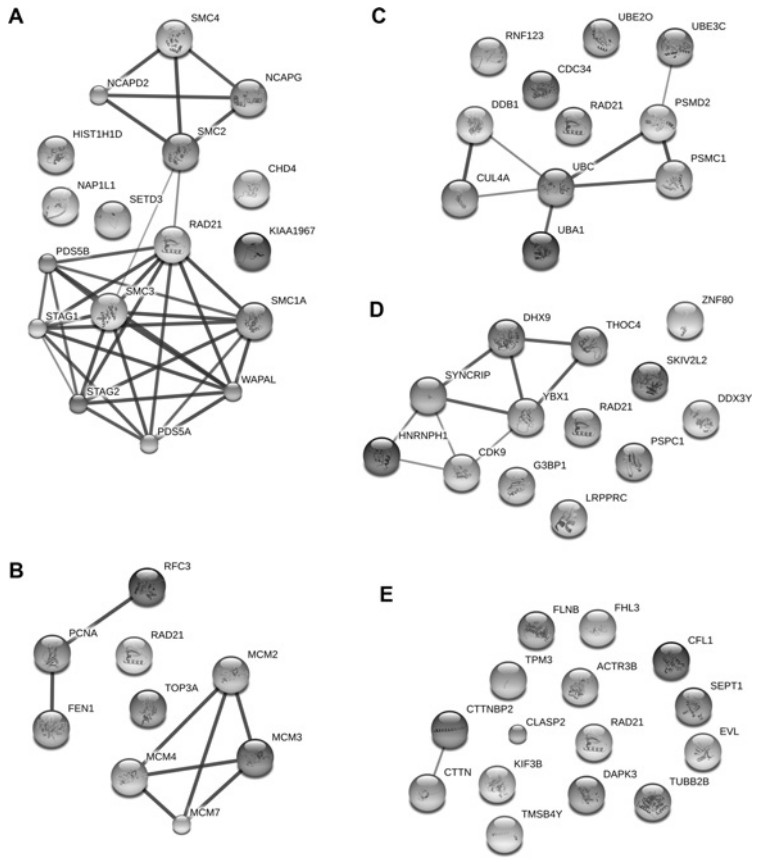

Figure 5 Selected clusters of RAD21 interactors

(**A**) Chromosome architecture and dynamics, (**B**) replication, (**C**) DDR and ubiquitination, (**D**) transcription and RNA metabolism, (**E**) cytoskeleton and cell motility. The clusters were generated from the composite list of interactors using DAVID, and each cluster was visualized using STRING. Interconnecting lines are based on known interactions; thicker lines represent stronger interactions. The interaction plot was generated by STRING using a setting of medium confidence (0.400). Proteins that are discussed in more detail are defined in the text or in the Tables, other protein abbreviations used in this Figure have not been defined.

is possible that several of the interactions reported in the present paper may be dynamic in reference to cell-cycle stages and may also change during the course of differentiation.

In summary, in the present study we have characterized a comprehensive protein interactome for the cohesin RAD21 and identified 112 proteins that interact with RAD21. These proteins function in diverse sets of pathways and processes. However, the majority of the uncovered interactions with RAD21/cohesin await experimental validation, which will shed new light on the mechanism of cohesin function in global cellular pathways.

AUTHOR CONTRIBUTION

Debananda Pati conceived the idea and obtained the grant support. Debananda Pati, Anil Panigrahi and Nenggang Zhang designed the experiments. Debananda Pati, Anil Panigrahi, Nenggang Zhang and Subhendu Otta performed the experiments and analysed the data. Anil Panigrahi and Debananda Pati wrote the paper.

ACKNOWLEDGEMENTS

We thank Subhashree Pradhan (Baylor College of Medicine, Houston, TX, U.S.A.) for technical assistance. We thank Dr Lisa Wang for critically reading the paper prior to submission and Dr Betty Ligon for editing the text prior to submission.

FUNDING

This work was supported by the National Cancer Institute [grant number 1RO1 CA109478 (to D.P.)].

REFERENCES

1 Michaelis, C., Ciosk, R. and Nasmyth, K. (1997) Cohesins: chromosomal proteins that prevent premature separation of sister chromatids. Cell **91**, 35–45
2 Guacci, V., Koshland, D. and Strunnikov, A. (1997) A direct link between sister chromatid cohesion and chromosome condensation revealed through the analysis of MCD1 in *S. cerevisiae*. Cell **91**, 47–57
3 Haering, C. H., Lowe, J., Hochwagen, A. and Nasmyth, K. (2002) Molecular architecture of SMC proteins and the yeast cohesin complex. Mol. Cell **9**, 773–788
4 Losada, A., Yokochi, T., Kobayashi, R. and Hirano, T. (2000) Identification and characterization of SA/Scc3p subunits in the *Xenopus* and human cohesin complexes. J. Cell Biol. **150**, 405–416
5 Sumara, I., Vorlaufer, E., Gieffers, C., Peters, B. H. and Peters, J. M. (2000) Characterization of vertebrate cohesin complexes and their regulation in prophase. J. Cell Biol. **151**, 749–762
6 Peters, J. M., Tedeschi, A. and Schmitz, J. (2008) The cohesin complex and its roles in chromosome biology. Genes Dev. **22**, 3089–3114
7 Onn, I., Heidinger-Pauli, J. M., Guacci, V., Unal, E. and Koshland, D. E. (2008) Sister chromatid cohesion: a simple concept with a complex reality. Annu. Rev. Cell Dev. Biol. **24**, 105–129
8 Nasmyth, K. and Haering, C. H. (2009) Cohesin: its roles and mechanisms. Annu. Rev. Genet. **43**, 525–558
9 Waizenegger, I. C., Hauf, S., Meinke, A. and Peters, J. M. (2000) Two distinct pathways remove mammalian cohesin from chromosome arms in prophase and from centromeres in anaphase. Cell **103**, 399–410
10 Kueng, S., Hegemann, B., Peters, B. H., Lipp, J. J., Schleiffer, A., Mechtler, K. and Peters, J. M. (2006) Wapl controls the dynamic association of cohesin with chromatin. Cell **127**, 955–967
11 Zhang, N., Panigrahi, A. K., Mao, Q. and Pati, D. (2011) Interaction of sororin with polo-like kinase 1 mediates the resolution of chromosomal arm cohesion. J. Biol. Chem. **286**, 41826–41837

12 Hauf, S., Waizenegger, I. C. and Peters, J. M. (2001) Cohesin cleavage by separase required for anaphase and cytokinesis in human cells. Science **293**, 1320–1323
13 Xu, H., Yan, M., Patra, J., Natrajan, R., Yan, Y., Swagemakers, S., Tomaszewski, J. M., Verschoor, S., Millar, E. K., van der Spek, P. et al. (2011) Enhanced RAD21 cohesin expression confers poor prognosis and resistance to chemotherapy in high grade luminal, basal and HER2 breast cancers. Breast Cancer Res. **13**, R9
14 Meyer, R., Fofanov, V., Panigrahi, A., Merchant, F., Zhang, N. and Pati, D. (2009) Overexpression and mislocalization of the chromosomal segregation protein separase in multiple human cancers. Clin. Cancer Res. **15**, 2703–2710
15 Mukherjee, M., Ge, G., Zhang, N., Huang, E., Nakamura, L. V., Minor, M., Fofanov, V., Rao, P. H., Herron, A. and Pati, D. (2011) Separase loss of function cooperates with the loss of p53 in the initiation and progression of T- and B-cell lymphoma, leukemia and aneuploidy in mice. PLoS ONE **6**, e22167
16 Zhang, N., Ge, G., Meyer, R., Sethi, S., Basu, D., Pradhan, S., Zhao, Y. J., Li, X. N., Cai, W. W., El-Naggar, A. K. et al. (2008) Overexpression of Separase induces aneuploidy and mammary tumorigenesis. Proc. Natl. Acad. Sci. U.S.A. **105**, 13033–13038
17 Solomon, D. A., Kim, T., Diaz-Martinez, L. A., Fair, J., Elkahloun, A. G., Harris, B. T., Toretsky, J. A., Rosenberg, S. A., Shukla, N., Ladanyi, M. et al. (2011) Mutational inactivation of STAG2 causes aneuploidy in human cancer. Science **333**, 1039–1043
18 Porkka, K. P., Tammela, T. L., Vessella, R. L. and Visakorpi, T. (2004) RAD21 and KIAA0196 at 8q24 are amplified and overexpressed in prostate cancer. Genes Chromosomes Cancer **39**, 1–10
19 Yamamoto, G., Irie, T., Aida, T., Nagoshi, Y., Tsuchiya, R. and Tachikawa, T. (2006) Correlation of invasion and metastasis of cancer cells, and expression of the RAD21 gene in oral squamous cell carcinoma. Virchows Arch. **448**, 435–441
20 Xu, H., Tomaszewski, J. M. and McKay, M. J. (2011) Can corruption of chromosome cohesion create a conduit to cancer? Nat. Rev. Cancer **11**, 199–210
21 Merkenschlager, M. (2010) Cohesin: a global player in chromosome biology with local ties to gene regulation. Curr. Opin. Genet. Dev. **20**, 555–561
22 Liu, J., Zhang, Z., Bando, M., Itoh, T., Deardorff, M. A., Clark, D., Kaur, M., Tandy, S., Kondoh, T., Rappaport, E. et al. (2009) Transcriptional dysregulation in NIPBL and cohesin mutant human cells. PLoS Biol. **7**, e1000119
23 Dorsett, D. (2010) Gene regulation: the cohesin ring connects developmental highways. Curr. Biol. **20**, R886–R888
24 Kagey, M. H., Newman, J. J., Bilodeau, S., Zhan, Y., Orlando, D. A., van Berkum, N. L., Ebmeier, C. C., Goossens, J., Rahl, P. B., Levine, S. S. et al. (2010) Mediator and cohesin connect gene expression and chromatin architecture. Nature **467**, 430–435
25 Horsfield, J. A., Anagnostou, S. H., Hu, J. K., Cho, K. H., Geisler, R., Lieschke, G., Crosier, K. E. and Crosier, P. S. (2007) Cohesin-dependent regulation of Runx genes. Development **134**, 2639–2649
26 Watrin, E. and Peters, J. M. (2006) Cohesin and DNA damage repair. Exp. Cell Res. **312**, 2687–2693
27 Lehmann, A. R. (2005) The role of SMC proteins in the responses to DNA damage. DNA Repair (Amsterdam) **4**, 309–314
28 Strom, L., Lindroos, H. B., Shirahige, K. and Sjogren, C. (2004) Postreplicative recruitment of cohesin to double-strand breaks is required for DNA repair. Mol. Cell **16**, 1003–1015
29 Chen, F., Kamradt, M., Mulcahy, M., Byun, Y., Xu, H., McKay, M. J. and Cryns, V. L. (2002) Caspase proteolysis of the cohesin component RAD21 promotes apoptosis. J. Biol. Chem. **277**, 16775–16781
30 Sherwood, R., Takahashi, T. S. and Jallepalli, P. V. (2010) Sister acts: coordinating DNA replication and cohesion establishment. Genes Dev. **24**, 2723–2731
31 Ryu, M. J., Kim, B. J., Lee, J. W., Lee, M. W., Choi, H. K. and Kim, S. T. (2006) Direct interaction between cohesin complex and DNA replication machinery. Biochem. Biophys. Res. Commun. **341**, 770–775
32 Guillou, E., Ibarra, A., Coulon, V., Casado-Vela, J., Rico, D., Casal, I., Schwob, E., Losada, A. and Mendez, J. (2010) Cohesin organizes chromatin loops at DNA replication factories. Genes Dev. **24**, 2812–2822
33 Terret, M. E., Sherwood, R., Rahman, S., Qin, J. and Jallepalli, P. V. (2009) Cohesin acetylation speeds the replication fork. Nature **462**, 231–234
34 Pati, D., Zhang, N. and Plon, S. E. (2002) Linking sister chromatid cohesion and apoptosis: role of Rad21. Mol. Cell. Biol. **22**, 8267–8277
35 Pati, D., Meistrich, M. L. and Plon, S. E. (1999) Human Cdc34 and Rad6B ubiquitin-conjugating enzymes target repressors of cyclic AMP-induced transcription for proteolysis. Mol. Cell. Biol. **19**, 5001–5013
36 Zhang, N., Kuznetsov, S. G., Sharan, S. K., Li, K., Rao, P. H. and Pati, D. (2008) A handcuff model for the cohesin complex. J. Cell Biol. **183**, 1019–1031
37 Panigrahi, A. K., Zhang, N., Mao, Q. and Pati, D. (2011) Calpain-1 cleaves rad21 to promote sister chromatid separation. Mol. Cell. Biol. **31**, 4335–4347
38 Huang da, W., Sherman, B. T. and Lempicki, R. A. (2009) Systematic and integrative analysis of large gene lists using DAVID bioinformatics resources. Nat. Protoc. **4**, 44–57
39 Szklarczyk, D., Franceschini, A., Kuhn, M., Simonovic, M., Roth, A., Minguez, P., Doerks, T., Stark, M., Muller, J., Bork, P. et al. (2011) The STRING database in 2011: functional interaction networks of proteins, globally integrated and scored. Nucleic Acids Res. **39**, D561–D568
40 Yamaguchi, H., Durell, S. R., Chatterjee, D. K., Anderson, C. W. and Appella, E. (2007) The Wip1 phosphatase PPM1D dephosphorylates SQ/TQ motifs in checkpoint substrates phosphorylated by PI3K-like kinases. Biochemistry **46**, 12594–12603
41 Hakimi, M. A., Bochar, D. A., Schmiesing, J. A., Dong, Y., Barak, O. G., Speicher, D. W., Yokomori, K. and Shiekhattar, R. (2002) A chromatin remodelling complex that loads cohesin onto human chromosomes. Nature **418**, 994–998
42 Sowa, M. E., Bennett, E. J., Gygi, S. P. and Harper, J. W. (2009) Defining the human deubiquitinating enzyme interaction landscape. Cell **138**, 389–403
43 Gregson, H. C., Schmiesing, J. A., Kim, J. S., Kobayashi, T., Zhou, S. and Yokomori, K. (2001) A potential role for human cohesin in mitotic spindle aster assembly. J. Biol. Chem. **276**, 47575–47582
44 McCracken, S., Longman, D., Marcon, E., Moens, P., Downey, M., Nickerson, J. A., Jessberger, R., Wilde, A., Caceres, J. F., Emili, A. and Blencowe, B. J. (2005) Proteomic analysis of SRm160-containing complexes reveals a conserved association with cohesin. J. Biol. Chem. **280**, 42227–42236
45 Abramson, J., Giraud, M., Benoist, C. and Mathis, D. (2010) Aire's partners in the molecular control of immunological tolerance. Cell **140**, 123–135
46 Lleres, D., Denegri, M., Biggiogera, M., Ajuh, P. and Lamond, A. I. (2010) Direct interaction between hnRNP-M and CDC5L/PLRG1 proteins affects alternative splice site choice. EMBO Rep. **11**, 445–451
47 Camargo, L. M., Collura, V., Rain, J. C., Mizuguchi, K., Hermjakob, H., Kerrien, S., Bonnert, T. P., Whiting, P. J. and Brandon, N. J. (2007) Disrupted in schizophrenia 1 interactome: evidence for the close connectivity of risk genes and a potential synaptic basis for schizophrenia. Mol. Psychiatry **12**, 74–86
48 Dyer, M. D., Neff, C., Dufford, M., Rivera, C. G., Shattuck, D., Bassaganya-Riera, J., Murali, T. M. and Sobral, B. W. (2010) The human-bacterial pathogen protein interaction networks of *Bacillus anthracis*, *Francisella tularensis*, and *Yersinia pestis*. PLoS ONE **5**, e12089
49 Bhullar, J. and Sollars, V. E. (2011) YBX1 expression and function in early hematopoiesis and leukemic cells. Immunogenetics **63**, 337–350
50 Li, Z., Vizeacoumar, F. J., Bahr, S., Li, J., Warringer, J., Vizeacoumar, F. S., Min, R., Vandersluis, B., Bellay, J., Devit, M. et al. (2011) Systematic exploration of essential yeast gene function with temperature-sensitive mutants. Nat. Biotechnol. **29**, 361–367

Received 29 September 2011/5 December 2011; accepted 7 December 2011
Published as BJ Immediate Publication 7 December 2011, doi:10.1042/BJ20111745

Biochem. J. (2012) **442**, 661–670 (Printed in Great Britain) doi:10.1042/BJ20111745

online data

SUPPLEMENTARY ONLINE DATA
A cohesin–RAD21 interactome

Anil K. PANIGRAHI, Nenggang ZHANG, Subhendu K. OTTA and Debananda PATI[1]

Texas Children's Cancer Center, Department of Pediatric Hematology/Oncology, Baylor College of Medicine, 1102 Bates Avenue, Suite 1220 Houston, TX 77030, U.S.A.

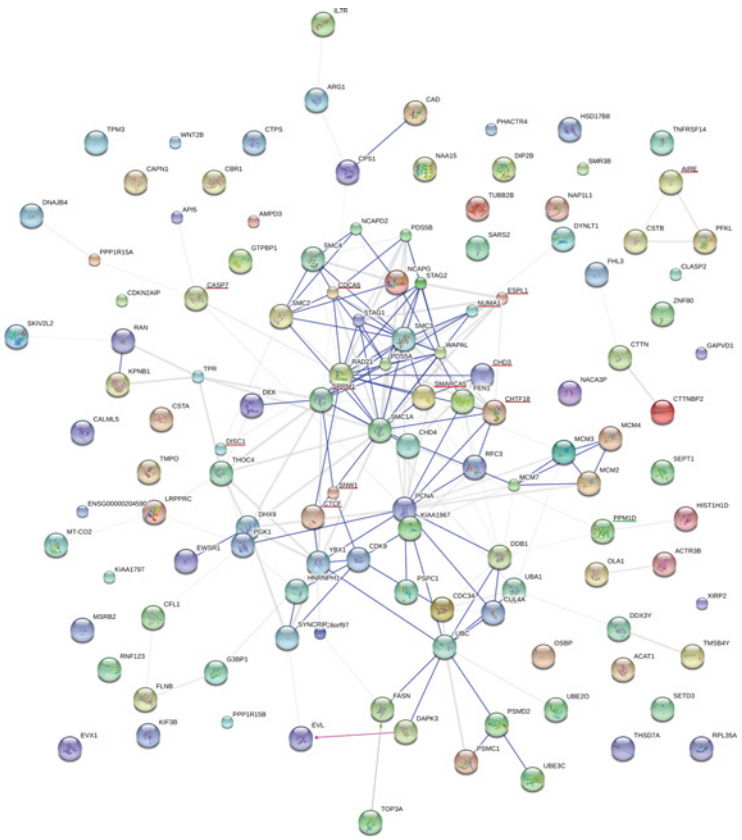

Figure S1 Composite RAD21 interactome as revealed by STRING

All RAD21-interacting proteins, identified from Y2H, immunopreciptation-coupled-MS and Myc–RAD21 affinity pull-down experiments were analysed together. Nodes underlined in red represent proteins known in the literature as RAD21 interactors, but not found in the present study; green underline (PPM1D) indicates a protein identified as a RAD21 interactor in a candidate approach, but not identified in any screen. Blue internodal lines indicate known binding, whereas grey lines indicate known or predicted functional interactions. The pink line represents experimentally verified enzymatic modification.

[1] To whom correspondence should be addressed (email pati@bcm.tmc.edu).

Table S1 RAD21 immunoprecipitation from MOLT-4 CE

Proteins	Description	Untreated	Etoposide	UniProt accession number
RAD21	Double-strand-break repair protein rad21 homologue	0	22	O60216
SMC1a	Structural maintenance of chromosomes protein 1A	0	43	Q14683
SMC3	Structural maintenance of chromosomes protein 3	0	42	Q9UQE7
SA2	Cohesin subunit SA-2	0	2	Q8N3U4
HIST1H1D	Histone H1 cluster c/d	0	6	P16402
EIF2S1	Eukaryotic translation initiation factor 2, subunit 1α	0	6	P05198
CSTA	Cystatin A	0	4	P01040
CCT8	Chaperonin-containing TCP1, subunit 8 (theta)	0	3	Q7Z759
ARG1	Arginase 1	0	3	P05089
EEF1D	Eukaryotic translation elongation factor 1δ	0	3	Q9BW34
DHX9	DEAH (Asp-Glu-Ala-His) box polypeptide 9, RNA helicase	0	2	Q58F26
KIF3B	Kinesin family member 3B	0	2	O15066
SFPQ	Splicing factor proline/glutamine-rich	4	11	P23246
A5PL27	Ceruloplasmin precursor	1	0	A5PL27
ITAM	Integrin α M precursor	1	0	P11215
TCF15	Basic helix-loop-helix transcription factor 15	1	0	Q12870
TRAIP	TRAF interacting protein	1	0	Q9BWF2
PIGR	Polymeric immunoglobulin receptor	5	0	P01833
C1QBP	Complement component 1, q subcomponent binding protein precursor	2	0	Q07021
ROA3	Heterogeneous nuclear ribonucleoprotein A3	1	0	P51991
YETS2	YEATS domain containing 2	1	0	Q9ULM3
STX10	Syntaxin 10	1	0	O60499
Q6IFM7	Olfactory receptor, family 1, subfamily E, member 2	1	0	Q6IFM7
PERM	Myeloperoxidase	24	0	P05164
ILEU	Serine (or cysteine) proteinase inhibitor, clade B (ovalbumin), member 1	4	0	P30740
TFG	TRK-fused	1	0	Q92734
CO3	Complement component 3 precursor	2	0	P01024
UB2L6	Ubiquitin-conjugating enzyme E2L 6 isoform 2	1	0	O14933
NPAT	Nuclear protein, ataxia-telangiectasia locus	1	0	Q14207
HNRPU	Heterogeneous nuclear ribonucleoprotein U isoform b	1	0	Q00839
Q7Z7Q0	Apolipoprotein B precursor	1	0	Q7Z7Q0
CLUS	Clusterin isoform 1	1	0	P10909
CCDC7	Coiled-coil domain containing 7	1	0	Q96M83
PDZD2	PDZ domain containing 2	1	0	O15018
APC4	Anaphase-promoting complex subunit 4	1	0	Q9UJX5
CATG	Cathepsin G preproprotein	6	0	P08311
S10A9	S100 calcium-binding protein A9	3	0	P06702
H4	Histone cluster 2, H4b	2	0	P62805
CAP7	Azurocidin 1 preproprotein	3	0	P20160
Q7Z4P3	Ubiquitin and ribosomal protein L40 precursor	1	0	Q7Z4P3
CALL3	Calmodulin-like 3	5	0	P27482
H15	Histone cluster 1, H1b	5	0	P16401
H2AJ	H2A histone family, member J	1	0	Q9BTM1
ECP	Ribonuclease, RNase A family, 3 (eosinophil cationic protein)	3	0	P12724
AHSP	Erythroid-associated factor	1	0	Q9NZD4

Table S2 Immunoprecipitation of RAD21 from HeLa NEs and CEs

Protein	Description	NE	CE	Uniprot accession number
RAD21	Double-strand-break repair protein rad21 homologue	31	0	O60216
SMC1A	Structural maintenance of chromosomes protein 1A	11	0	Q14683
SMC3	Structural maintenance of chromosomes protein 3	6	0	Q9UQE7
SA1	Cohesin subunit SA-1	2	0	Q8WVM7
SA2	Cohesin subunit SA-2	2	0	Q8N3U4
PDS5A	Scc-112 protein	2	0	Q29RF7
WAPAL/Wapl	Wings apart-like homologue (*Drosophila*)	12	0	Q7Z5K2
LRPPRC	Leucine-rich PPR motif-containing protein	4	0	P42704
Nap1L1	Nucleosome assembly protein 1-like 1	8	0	P55209
RFC3	Replication factor C subunit 3	2	0	P40938
DNA-PK	DNA-activated protein kinase catalytic subunit	5	1	P78527
NCAPG	Condensin Component	2	0	Q9BPX3
TPR	Nucleoprotein TPR	3	0	P12270
CPS1	Carbamoyl-phosphate synthase	6	0	P31327
HSP90AA	Heat-shock protein 90 kDa α (cytosolic)	0	20	P07900
HSP90AB	Heat-shock protein HSP 90-β	0	16	P08238
TRAP1	TNFR-associated protein 1	0	2	Q12931
TCP-1 and associated chaperonins (CCT3-8)		0	>20	

Table S3 Proteins identified from Myc–RAD21 pull-down analysis

Protein	Description	UniProt accession number	Rad21*
RAD21	Double-strand-break repair protein rad21 homologue	O60216	27
UBC	RPS27A, UBB ubiquitin and ribosomal protein S27a precursor	Q5RKT7	18
EIF3A	Eukaryotic translation initiation factor 3 subunit A	Q14152	17
YBX1	Nuclease-sensitive element-binding protein 1	P67809	15
RPS3	40S ribosomal protein S3	P23396	12
GAPVD1	Isoform 6 of GTPase-activating protein and VPS9 domain-containing protein 1	Q14C86	12
RPL5	60S ribosomal protein L5	P46777	11
EIF3CL	EIF3C eukaryotic translation initiation factor 3 subunit C	Q99613	11
GTPBP1	GTP-binding protein 1	O00178	9
UBE2O	Ubiquitin-conjugating enzyme E2 O	Q9C0C9	10
RPS4X	40S ribosomal protein S4, X isoform	P62701	9
EIF4A1	SNORA67 eukaryotic initiation factor 4A-I	P60842	11
EIF2S3	Eukaryotic translation initiation factor 2 subunit 3	P41091	8
HSP90AA1	Heat shock 90kDa protein 1, α isoform 1	P07900	9
RPS18	LOC100130553 40S ribosomal protein S18	P62269	7
FASN	Fatty acid synthase	P49327	8
CAD	Protein	P27708	8
EIF3B	Isoform 1 of eukaryotic translation initiation factor 3 subunit B	P55884	8
EIF4G2	cDNA FLJ59571, highly similar to eukaryotic translation initiation factor 4γ2	B4DZF2	7
TUBB2C	Tubulin β-2C chain	P68371	6
RPS14	40S ribosomal protein S14	P62263	6
SMC2	Isoform 1 of structural maintenance of chromosomes protein 2	O95347	7
EIF4G1	EIF4G1 protein	Q04637	6
CTPS	CTP synthase 1	P17812	6
CCT7	T-complex protein 1 subunit η	Q99832	6
RNF123	Isoform 1 of E3 ubiquitin–protein ligase RNF123	Q5XPI4	6
PFKL	Isoform 1 of 6-phosphofructokinase, liver type	P17858	6
RPS2	40S ribosomal protein S2	P15880	5
RPL23A	60S ribosomal protein L23a	P62750	5
HSD17B8	Oestradiol 17-β-dehydrogenase 8	Q92506	4
SYNCRIP	Isoform 1 of heterogeneous nuclear ribonucleoprotein Q	O60506	4
SEPT1	Septin-1	Q8WYJ6	4
RPS25	40S ribosomal protein S25	P62851	4
SMC4	Isoform 2 of structural maintenance of chromosomes protein 4	Q9NTJ3	5
RPS16	40S ribosomal protein S16	P62249	5
RPS7	40S ribosomal protein S7	P62081	5
CDKN2AIP	CDKN2A-interacting protein	Q7Z335	2
PSPC1	Isoform 1 of paraspeckle component 1	Q8WXF1	3
RPS26P11	Putative 40S ribosomal protein S26-like 1	Q5JNZ5	3
RPL11	Isoform 1 of 60S ribosomal protein L11	P62913	3
DNAJB4	DnaJ homologue subfamily B member 4	Q9UDY4	4
SARS2	Seryl-tRNA synthetase, mitochondrial	Q9NP81	3
SKIV2L2	Superkiller viralicidic activity 2-like 2	P42285	4
CBR1	Carbonyl reductase [NADPH] 1	P16152	4
EIF2S1	Eukaryotic translation initiation factor 2 subunit 1	P05198	4
API5	Isoform 2 of apoptosis inhibitor 5	Q9BZZ5	4
RPS19	40S ribosomal protein S19	P39019	4
RPS15A	40S ribosomal protein S15a	P62244	4
RPS20	40S ribosomal protein S20	P60866	4
RPS13	40S ribosomal protein S13	P62277	4
NCAPD2	Condensin complex subunit 1	Q15021	4
RPS11	40S ribosomal protein S11	P62280	4
RPS3A	40S ribosomal protein S3a	P61247	4
DDX3X	ATP-dependent RNA helicase DDX3X	O00571	5
RPL23	60S ribosomal protein L23	P62829	4
ACTR3	Actin-related protein 3	P61158	2
CLASP2	Isoform 2 of CLIP-associating protein 2	O75122	2
CDK9	Isoform 1 of cell division protein kinase 9	P50750	2
RAN	RAN GTP-binding nuclear protein Ran	P62826	2
FEN1	Flap endonuclease 1	P39748	2
RPS6	40S ribosomal protein S6	P62753	2
PSMC1	26S protease regulatory subunit 4	P62191	2
TOP3A	Isoform long of DNA topoisomerase 3-α	Q13472	2
DIP2B	Isoform 1 of disco-interacting protein 2 homologue B	Q9P265	2
EIF4B	cDNA FLJ54492, highly similar to eukaryotic translation initiation factor 4B	B4DRM3	2
NCAPG	Condensin complex subunit 3	Q9BPX3	3
ACAT1	Acetyl-CoA acetyltransferase, mitochondrial	P24752	3
RPL6	60S ribosomal protein L6	Q02878	3

Table S3 Continued

Protein	Description	UniProt accession number	Rad21*
RPL22	60S ribosomal protein L22	P35268	3
PSMD2	26S proteasome non-ATPase regulatory subunit 2	Q13200	3
CAPN1	Calpain-1 catalytic subunit	P07384	2
NACA3P	Nascent polypeptide-associated complex subunit α	Q13765	2
SETD3	Isoform 1 of SET domain-containing protein 3	Q86TU7	2
RPL30	60S ribosomal protein L30	P62888	2
DDB1	DNA damage-binding protein 1	Q16531	2
CCT2	T-complex protein 1 subunit β	P78371	2
AMPD3	Isoform 1B of AMP deaminase 3	Q01432	2
GNL1	HSR1 protein	Q0EFC6	2
CUL4A	Isoform 1 of cullin-4A	Q13619	2
KIAA1797	Uncharacterized protein KIAA1797	Q5VW36	2
OLA1	Isoform 3 of Obg-like ATPase 1	Q9NTK5	2
EIF3D	Eukaryotic translation initiation factor 3 subunit D	O15371	2
EIF3F	HCG1784554, isoform CRA_a	B3KSH1	2
RPS10	40S ribosomal protein S10	P46783	2
EVL	Isoform 2 of Ena/VASP-like protein	Q9UI08	2
RPL13P12	Similar to RPL13 protein	IPI00397611 (+ 1)	2
CTTN	Src substrate cortactin	Q14247	2
NARG1	Isoform 2 of NMDA receptor-regulated protein 1	Q9BXJ9	2
UBE3C	Isoform 2 of ubiquitin-protein ligase E3C	Q15386	2
RPL22L1	60S ribosomal protein L22-like 1	Q6P5R6	2
RPS5	40S ribosomal protein S5	P46782	2
OSBP	Isoform 1 of oxysterol-binding protein 1	P22059	2
RPL17	LOC100133931 60S ribosomal protein L17	P18621	2
CCT3	Chaperonin containing TCP1, subunit 3 isoform b	Q5SZY0	2
EIF3I	Eukaryotic translation initiation factor 3 subunit I	Q13347	2
RPS17	40S ribosomal protein S17	P08708	2
G3BP1	Ras GTPase-activating protein-binding protein 1	Q13283	2

*Number of peptides obtained from the Myc–RAD21 matrix. No peptides for these proteins were obtained from the Mock (Myc–agarose) beads.

Received 29 September 2011/5 December 2011; accepted 7 December 2011
Published as BJ Immediate Publication 7 December 2011, doi:10.1042/BJ20111745